Functionalization of whole-cell bacterial reporters with magnetic nanoparticles

Dayi Zhang,[1†] Rawil F. Fakhrullin,[1,2,3†]
Mustafa Özmen,[3,4] Hui Wang,[5] Jian Wang,[6]
Vesselin N. Paunov,[3] Guanghe Li[7] and
Wei E. Huang[1*]

[1]*Kroto Research Institute, University of Sheffield, Broad Lane, Sheffield S3 7HQ, UK.*
[2]*Biomaterials and Nanomaterials Group, Department of Biochemistry, Kazan (Idel buye) Federal University, Kreml uramı 18, Kazan, 420008, Republic of Tatarstan.*
[3]*Surfactant and Colloid Group, Department of Chemistry, University of Hull, Hull HU6 7RX, UK.*
[4]*Selcuk University, Science Faculty, Department of Chemistry, 42075 Campus, Konya, Turkey.*
[5]*Centre for Ecology and Hydrology, Oxford, Mansfield Road, Oxford OX1 3SR, UK.*
[6]*Beijing Genomics Institute (BGI)-Shenzhen, Main Building, Beishan Industrial Zone, Yantian District, Shenzhen 518083, China.*
[7]*Department of Environmental Science & Engineering, Tsinghua University, Beijing 100084, China.*

Summary

We developed a biocompatible and highly efficient approach for functionalization of bacterial cell wall with magnetic nanoparticles (MNPs). Three *Acinetobacter baylyi* ADP1 chromosomally based bioreporters, which were genetically engineered to express bioluminescence in response to salicylate, toluene/xylene and alkanes, were functionalized with 18 ± 3 nm iron oxide MNPs to acquire magnetic function. The efficiency of MNPs functionalization of *Acinetobacter* bioreporters was 99.96 ± 0.01%. The MNPs-functionalized bioreporters (MFBs) can be remotely controlled and collected by an external magnetic field. The MFBs were all viable and functional as good as the native cells in terms of sensitivity, specificity and quantitative response. More importantly, we demonstrated that salicylate sensing MFBs can be applied to sediments and garden soils, and semi-quantitatively detect salicylate in those samples by discriminably recovering MFBs with a permanent magnet. The magnetically functionalized cells are especially useful to complex environments in which
the indigenous cells, particles and impurities may interfere with direct measurement of bioreporter cells and conventional filtration is not applicable to distinguish and harvest bioreporters. The approach described here provides a powerful tool to remotely control and selectively manipulate MNPs-functionalized cells in water and soils. It would have a potential in the application of environmental microbiology, such as bioremediation enhancement and environment monitoring and assessment.

Introduction

Bacterial cells can be used as chassis for synthetic biology, which can be genetically reprogrammed to undertake novel tasks such as sensing specific chemicals, producing proteins, drugs and biofuels (Ro *et al.*, 2006; Atsumi *et al.*, 2009), acting as multi-enzyme biocatalysts, generating logic circuits (Silva-Rocha and de Lorenzo, 2008) and demonstrating oscillating patterns (Stricker *et al.*, 2008; Danino *et al.*, 2010). Apart from genetic modification, nanoparticles (NPs) provide additional toolboxes to modify bacterial cells. NPs exhibit new and interesting properties (e.g. quantum entanglement, unique photonic, electronic and catalytic properties) that bulk materials lack (Whitesides, 2005). NPs functionalized with various molecules are able to access the cell membranes or enter into the cytoplasm (Katz and Willner, 2004). Bacteria were also used as templates for direct deposition of gold NPs in order to produce novel microelectronic devices (Berry and Saraf, 2005) and therapeutic entities (Kuo *et al.*, 2008). The combination of nanotechnology and microbiology endows bacterial cells with novel functions which are supposed to have many potential applications in medicine, biofuel production, environmental monitoring and bioremediation (Katz and Willner, 2004).

Magnetic nanoparticles (MNPs), as a versatile tool for the remote manipulation and control, can be used to functionalize not only inorganic and organic microparticles (i.e. microcrystals and hollow polymer microcapsules) (Dyab *et al.*, 2009; Fakhrullin *et al.*, 2009), but also yeast cells (Fakhrullin *et al.*, 2010). An advantage of MNPs functionalization of living cells is that it enables to remotely control and selectively manipulate cells *in vivo*. This 'action at distance' property provides a powerful tool to investigate cell–cell and cell–chemical interactions.

Conventional functionalization of bacterial cells with MNPs may have an adverse effect on their viability and cell functions. A major challenge is to keep bacteria alive and physiologically functional after MNPs functionalization process. MNPs have been used to magnetically functionalize yeast cells (Safarik *et al.*, 2007; Safarikova *et al.*, 2009), but extensive treatment with acids and cells exposure to cytotoxic reagents significantly reduced viability of those yeast cells. Here we describe a generic biocompatible approach for functionalization of bacterial cells with MNPs. To the best of our knowledge, there have been no reports yet for magnetic functionalization of prokaryotic cells with MNPs. We employed the biocompatible approach to attach 18 nm MNPs onto *Acinetobacter baylyi* ADP1 chromosomally based bioreporters, which are able to sense salicylate, toluene/xylene and alkanes (Huang *et al.*, 2005; 2008; D. Zhang, Y. He, J. Zhao, L. Wu, J. Wang, H. Wang and W.E. Huang, in preparation). The efficiency of MNPs functionalization to the bioreporters was $99.96 \pm 0.01\%$ and MNPs-functionalized bioreporters (MFBs) were viable and functional as good as the native cells. More importantly, we demonstrated that MFBs can be applied to semi-quantitatively detect salicylate present in sediments and garden soils.

Results

Characterization of poly(allylamine hydrochloride) (PAAH)-stabilized MNPs and MFBs

In this article we used poly(allylamine hydrochloride) (PAAH)-stabilized MNPs to functionalize living bacteria. PAAH is a positively charged, non-toxic and biocompatible polymer which has been reported to strongly adhere to the cell surface (Diaspro *et al.*, 2002; Krol *et al.*, 2005; Veerabadran *et al.*, 2007; Fakhrullin and Paunov, 2009; Zamaleeva *et al.*, 2010) and has been used as a component of layer-by-layer polyelectrolyte nanocomposite multilayers and hollow capsules (Decher, 1997; Ai *et al.*, 2002; Andreeva *et al.*, 2007; Shutava *et al.*, 2009). We employed a modified approach to functionalize bacterial cells, including repeatedly separation and purification of PAAH-stabilized MNPs. The aqueous dispersion of MNPs was stable (no aggregation was observed at least during 6 months), and PAAH-stabilized MNPs dispersed in pure water have shown good biocompatibility and cell-friendly properties.

The concentration of MNPs in aqueous solution was determined to be 0.4 mg ml^{-1}. The transmission electron microscopy (TEM) image (Fig. 1A) shows that the MNPs had almost spherical shape and the size distribution was around 18 ± 3 nm, which is consistent with the previous reports (Fakhrullin *et al.*, 2010; García-Alonso *et al.*, 2010). Zeta-potential of PAAH-stabilized MNPs in water was positive (38 ± 6 mV) which makes these MNPs

readily adhesive to bacterial cells which usually bear a negative surface charge. The magnetic behaviour of MFBs is demonstrated in Movie S1 (*Supporting information*) which shows spatial manipulation of MFBs (*Acinetobacter* ADPWH_lux) with a permanent magnet and the MFBs were 'flipping' following the magnetic field. Cells functionalized with MNPs had a strong magnetic property and can be readily collected. Figure 1B shows that almost all MFBs (*Acinetobacter* ADPWH_lux) were assembled to the magnetic side of a vial so that originally turbid cell suspension became transparent and clear within 10 min. It indicates that the MNPs functionalization endowed *Acinetobacter* cells a magnetotaxis-like function. To examine the deposition and distribution of the PAAH-stabilized MNPs on the cells, we used MNPs stabilized with FITC-labelled PAAH to functionalize *Acinetobacter* ADPWH_lux which were visualized using epifluorescent microscopy. Figure 1C shows the uniform distribution of the fluorescently labelled MNPs on each cell, indicating the even functionalization of the MNPs on *Acinetobacter* cells. The TEM image of thin-sectioned MNPs-functionalized *Acinetobacter* strain ADPWH_lux indicates that the MNPs adhered to the cell surface (Fig. 1D). After examining the magnified TEM images we found that the MNPs exclusively attached to cell outer wall and no MNPs were found in cytoplasm (Fig. 1E). In addition, energy-dispersive X-ray (EDX) spectra of the MFBs (Fig. 1F) and scanning electron microscopy (SEM) images (Fig. S1) confirmed the presence of iron NPs on the cell wall.

Functionalization efficiency and viability of MFBs

The efficiency of MNPs functionalization was estimated by plate counting of magnetic and non-magnetic bioreporter ADPWH_lux. Magnetic ADPWH_lux were fractions from magnetic adhesive cells collected by a permanent magnet; while non-magnetic cells were those remaining in water phase after magnetic attraction (Fig. S2). The populations of the magnetic ADPWH_lux were $2.22 \pm 0.10 \times 10^8$ colony-forming unit (cfu) ml^{-1} and the non-magnetic cells were $8.00 \pm 0.51 \times 10^4$ cfu ml^{-1} (Fig. S2), indicating the efficiency of magnetic functionalization was $99.96 \pm 0.01\%$. Since the populations of magnetic ADPWH_lux were estimated by colony-counting on agar plates, it suggested that the cells were still viable and the MNPs functionalization process was biocompatible. The high level of viability can be explained by the inability of PAAH-stabilized MNPs to enter the cytoplasm (Fig. 1E). Furthermore, we examined the division and growth of ADPWH_lux MFBs. Figure S3 shows that the fractions of 'free' (non-magnetic) cells gradually increased from original 0 to 12% during 120 min incubation at 30°C, which confirmed that MFBs were able to divide and grow as usual. Multiple generations of cell divisions may reduce
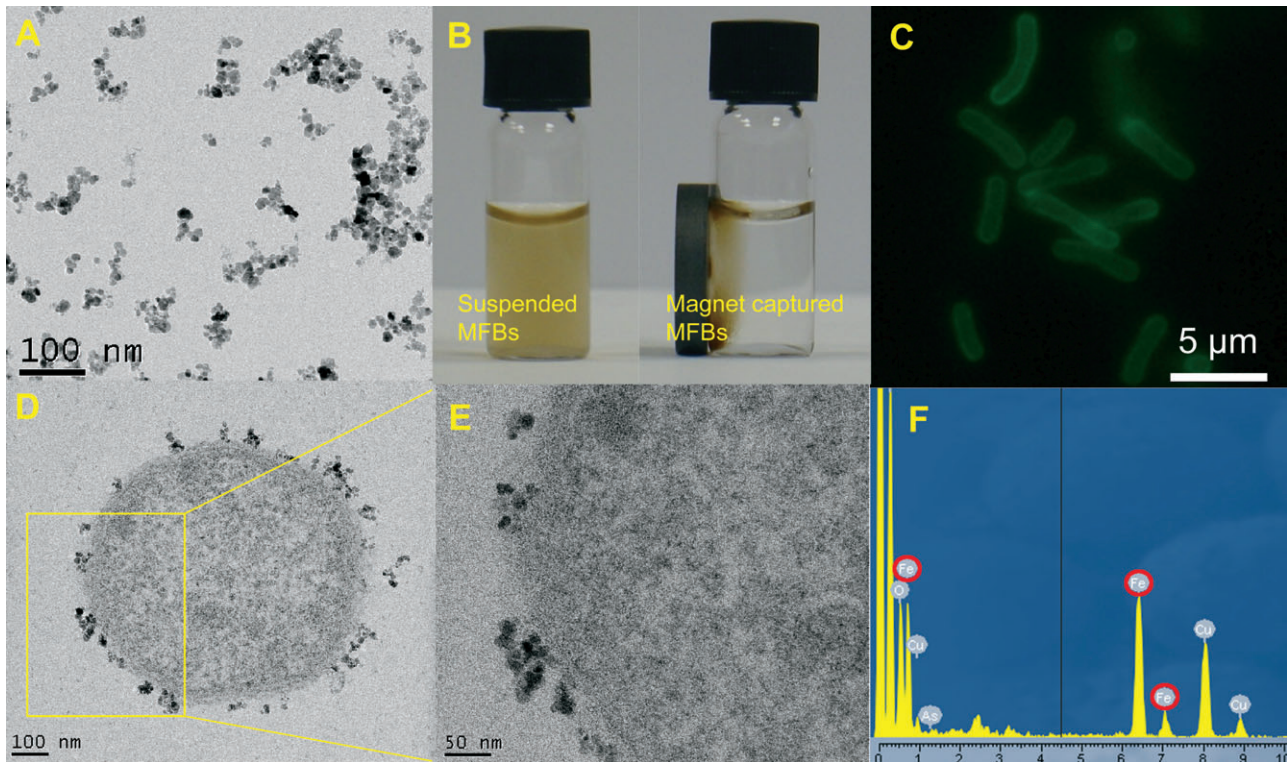
Fig. 1. Characterization of MNPs and MFBs.
A. A typical TEM image of aqueous magnetic nanoparticles stabilized with PAAH.
B. Magnetic controls on ADPWH_lux MFBs. Originally suspended MFBs (left) were attracted to the side of a permanent magnet (right) after 10 min.
C. Epifluorescent microscopy image of cells of *Acinetobacter* strain ADPWH_lux functionalized with MNPs stabilized with FITC-PAAH.
D and E. TEM images of the thin-sectioned ADPWH_lux MFBs.
F. EDX spectra obtained from the cell shown in (D). Note the iron peaks highlighted by red. The copper signal originates from the copper TEM grid which was used during TEM imaging.

the number of MNPs on daughter cells and therefore decreased cells magnetic adherence and became 'free' in aqueous phase, but taking into account the suggested applications, this should not affect the functionality of the MFBs.

Functionality of MFBs

To evaluate the impact of magnetic functionalization on bacterial cellular functionalities, we compared MFBs and native bioreporters for their biosensing performance. In this study, we examined three chromosomally based *Acinetobacter* bioreporters: ADPWH_lux, ADPWH-Pu-lux-xylR and ADPWH_alk, which are able to sense salicylate, toluene/xylenes and alkanes separately (Huang *et al.*, 2005; 2008; D. Zhang, Y. He, J. Zhao, L. Wu, J. Wang, H. Wang and W.E. Huang, in preparation). To induce native bioreporters, the inducers (salicylate, toluene/xylenes or alkanes) should pass through the cell membranes of the bioreporters, enter into the cytoplasm and interact with regulatory proteins (SalR, XylR or AlkR) which will undergo conformational change and activate the associ-

ated promoters to express reporter genes *luxCDABE* and show bioluminescence (Huang *et al.*, 2005; 2008; D. Zhang, Y. He, J. Zhao, L. Wu, J. Wang, H. Wang and W.E. Huang, in preparation). Because the MNPs functionalization affected cell absorbance property, it would be appropriate to use bioluminescence intensity per cell for the estimation of relative bioluminescence. Therefore, the cell turbidity OD_{600} was converted to cell population (MFBs and native cells) by using the calibration curves plotted in Fig. S4. The results show that dynamic induction patterns of ADPWH_lux MFBs (Fig. 2A) were similar to that of the native cells (Fig. 2B).

As MFBs can divide and escape magnetic controlling (Fig. S2), we decided to perform cell induction at 60 min to evaluate the sensitivity of MFBs. Figure 3A shows that the sensitivity of ADPWH_lux MFBs remained unchanged and the salicylate detection limit was still 50 nM ($P = 0.014$). The relative response ratios (bioluminescence ratio between induced and non-induced cells) of MFBs were just slightly lower than that of the native (control) cells (Fig. 3A). Figure 1D suggests that MNPs attached area was less than 10% coverage of the cell
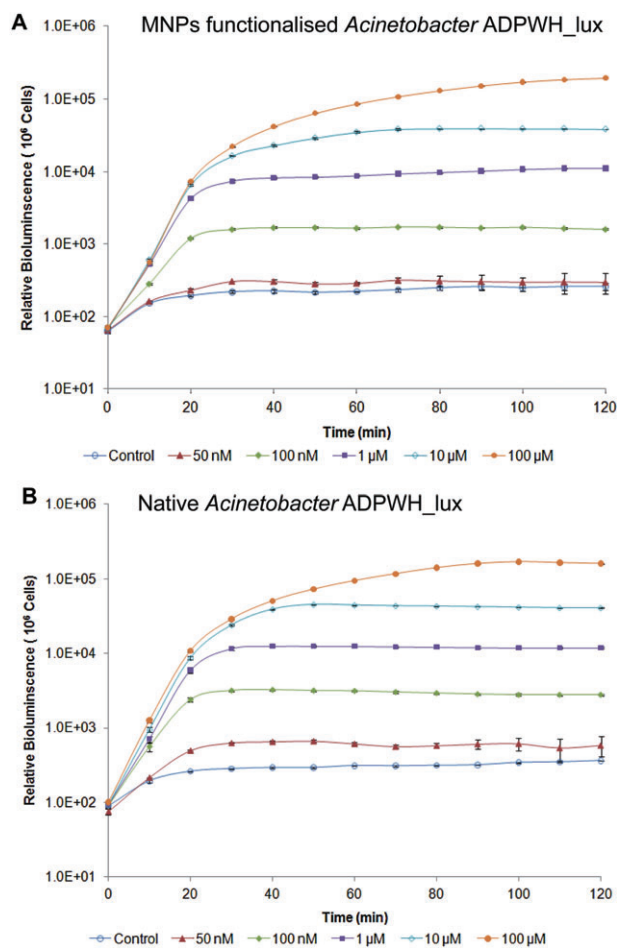
Fig. 2. Comparison of dynamic sensing behaviour of MNPs-functionalized (A) and native *Acinetobacter* ADPWH_lux (B). Cells are induced by different concentrations of salicylate.

surface. Therefore, MNPs' effect on bioreporters performance should not be severe.

Apart from the water-soluble inducer (salicylate), we also examined the effect of other inducers (toluene and alkanes) on MFBs. Toluene and alkanes were supposed to have different inducer transport patterns which may be affected by MNPs functionalization on cell wall, since toluene is a cell membrane solvent and alkanes are unpolar compounds. Figure 3B and C shows that ADPWH-Pu-lux-xylR and ADPWH_alk MFBs can be induced by toluene and alkanes (octane, dodecane, tetradecane and octadecane), and magnetic functionalization had little effect on the bioreporter induction. Figure 3D shows that octadecane (saturated in water) was able to induce ADPWH_alk ($P < 0.05$) but failed to induce ADPWH_lux and ADPWH-Pu-lux-xylR. The addition of octadecane to the inducer (salicylate or toluene) did not induce further bioluminescence from ADPWH_lux or ADPWH-Pu-lux-xylR (Fig. 3D). Collectively, these results indicate that ADPWH_alk was indeed induced by alkanes (e.g. octadecane) and preclude the possibility that ADPWH_alk induction was due to alkanes (e.g. octadecane) being used as substrates for bioluminescence reaction. Overall, we conclude that the bioreporter functionality was not hindered by the magnetic functionalization with MNPs

Application of MFBs to the detection of chemicals in sediments and soils

As a proof of concept, we applied ADPWH_lux MFBs to detect salicylate in sediments and garden soils which contained salicylate with different concentrations (Fig. 4). MFBs were selectively recovered from the sediment and soil samples by a permanent magnet after 20 min induction. It is notable that MFBs have already shown different bioluminescent intensities at the first measurement time point (Fig. 4), which suggests that ADPWH_lux MFBs were induced in sediments and soils instead of late process. The first bioluminescence reading time in Fig. 4 was the time after 20 min induction and about 15 min sample process. The bioluminescent intensities of ADPWH_lux MFBs were proportional to salicylate concentrations in sediments and garden soils in the range of 0–14 mg per kilogram of sediments or soils (Figs 4 and S5), indicating ADPWH_lux MFBs cannot only detect the presence of salicylate but also semi-quantitatively estimate its concentrations in sediments or soils. The different performances of ADPWH_lux MFBs in sediments (Figs 4A and S5A) and soils (Figs 4B and S5B) may be due to the complexity of natural sediments and garden soils.

Discussion

In this study, iron oxide-based MNPs are considered due to their good biocompatibility (Corchero and Villaverde, 2009). We employed positively charged PAAH-stabilized superparamagnetic MNPs which are able to bind to the negatively charged bacterial cells and the MFBs can be easily re-dispersed after the removal of the magnetic field (Fig. 1). Such electrostatic interaction is able to functionalize MNPs to bacterial cells with extremely high efficiency. The MNPs used in this study can be attached to bacterial cells with an efficiency of 99.96%. The nanoscale MNPs (~18 nm) offer a strong magnetic property to bacterial cells and enable to separate cells more efficiently. The MFBs can be spatially controlled by an external magnetic field (Movie S1 and Fig. 1B) without jeopardizing the cellular viability and functionality. We suggest the approach using PAAH-stabilized MNPs can also be employed to immobilize other types of NPs (such as Au and Ag NPs) onto bacterial cells. In addition, potentially the MNPs are able to provide cells with catalytic functions because magnetite (Fe_3O_4) NPs were recently
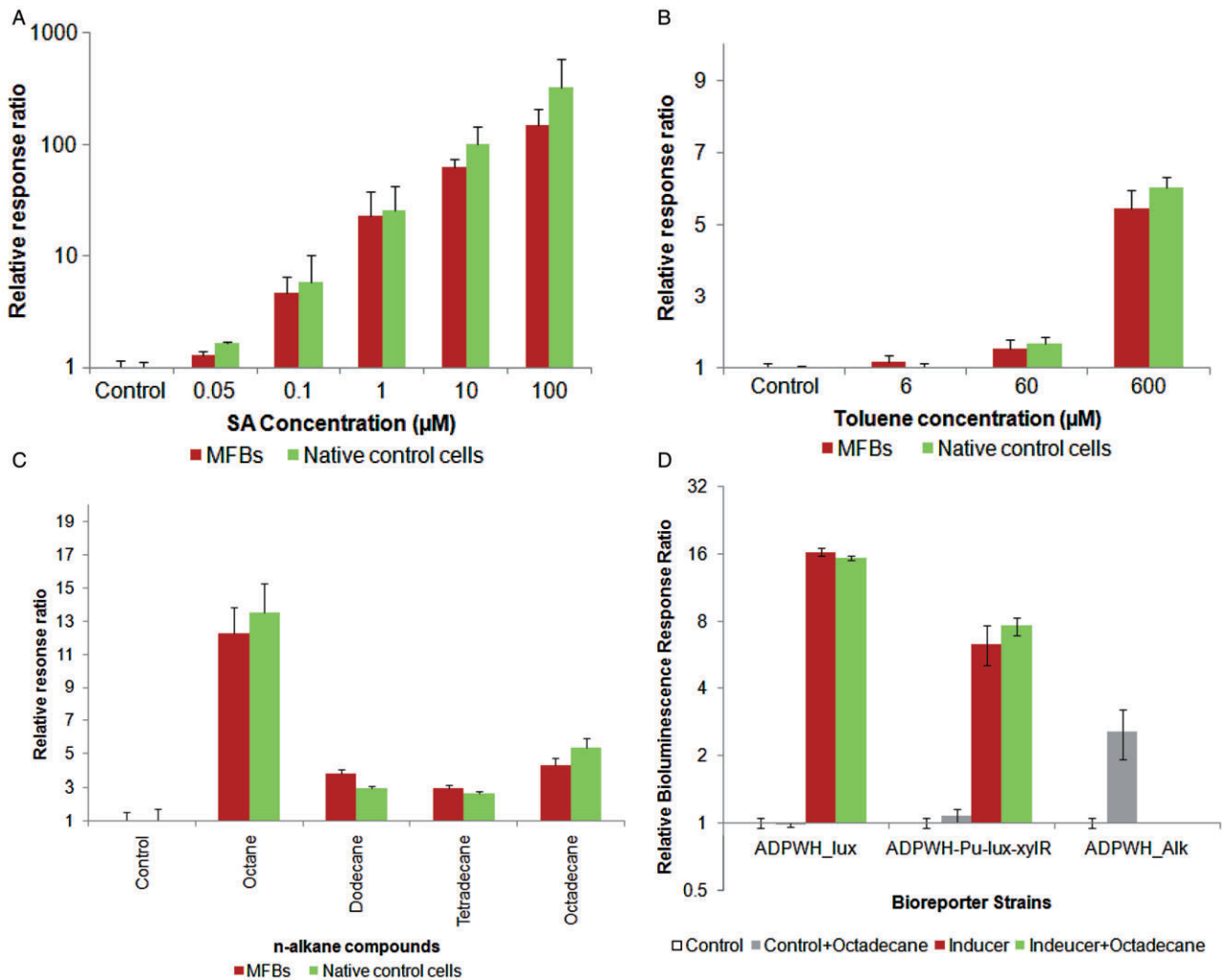
Fig. 3. Comparison of the sensing behaviour of MFBs of *Acinetobacter* bioreporters: salicylate (ADPWH_lux), toluene (ADPWH-Pu-lux-xylR) and alkanes (ADPWH_Alk) after 60 min incubation at 30°C.

A. Relative response ratio of MFBs and native ADPWH_lux induced by 50 nM–100 μM salicylate.

B. Relative response ratio of toluene bioreporters induced by 6–600 μM toluene in comparison with non-induced controls. The *P*-values are less than 0.05 except toluene concentration was 6 μM.

C. Relative response ratio of alkanes native bioreporters and MFBs induced by alkanes with different carbon chains in comparison with non-induced controls.

D. Relative response ratio of salicylate (ADPWH_lux), toluene (ADPWH-Pu-lux-xylR) and alkanes (ADPWH_Alk) MFBs induced by saturated octadecane, and 1 μM salicylate or 300 μM toluene in the presence or absence of saturated octadecane.

discovered to possess peroxidase-like activity (Gao *et al.*, 2007; Wei and Wang, 2008). MNPs can also be used as contrast enhancing agents in magnetic resonance imaging (MRI) (Gao *et al.*, 2009) and even to switch on the ion channels in cell membrane (Dobson, 2008).

Here we have proved the concept that MFBs can be used to detect chemical compounds in sediments and soils. The functionalization of MNPs to cells is especially useful in complex environments in where the indigenous cells and particles may interfere with direct measurement of bioreporters; or where filtration or other method is not applicable to track and find bioreporters. The MFBs can be regarded as millions of remotely controllable micro-

biosensing robots that are able to probe the chemical or biological information in wastewater, groundwater or complex environment where scientific instruments cannot readily access to. Those bioreporters can be simply re-collected for further analysis after exposing to contaminated environment. MNPs cell functionalization potentially can be used to magnetically modify contaminant degraders which can be remotely controlled to spatially and temporally interact with contaminants and enhance bioremediation. MNPs functionalization also offers a simple and easy way to spatially arrange and temporally control cells to make special patterns such as biofilms or multicellular structures.

A

B
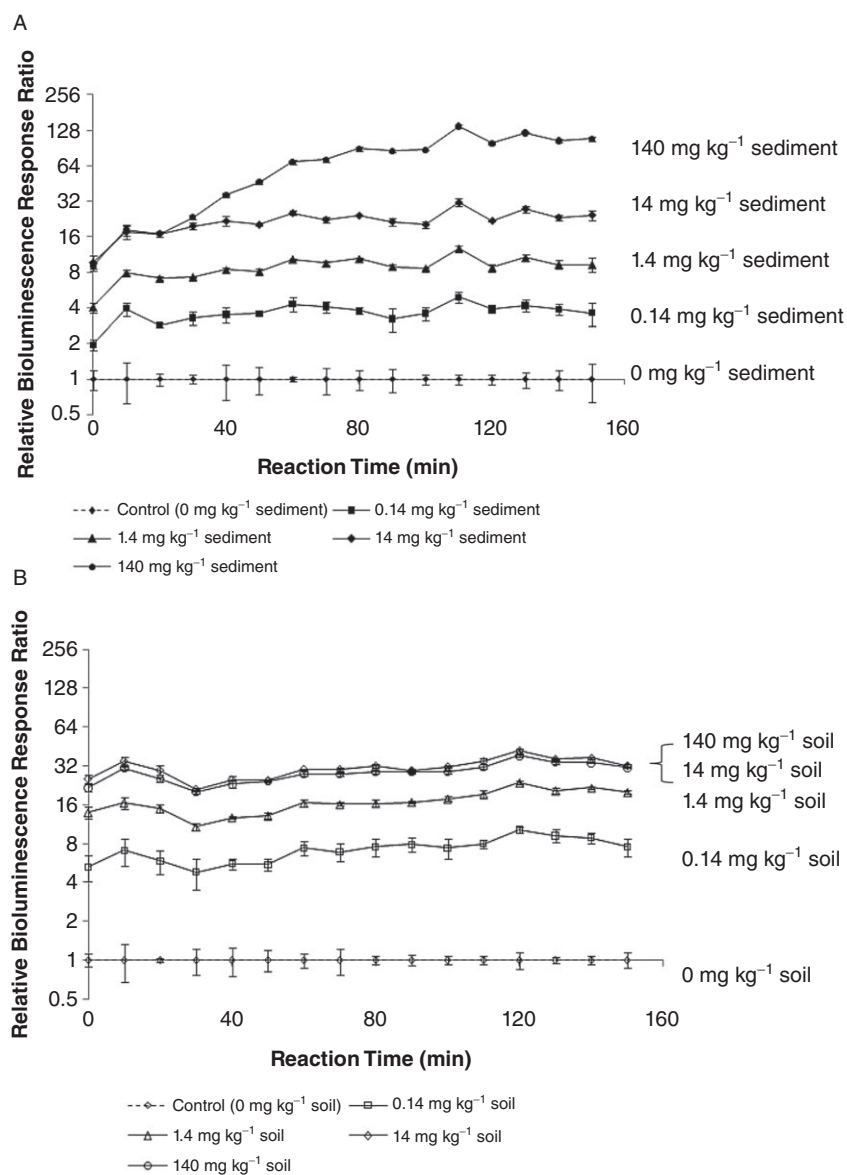
Fig. 4. ADPWH_lux MFBs detecting salicylate with different concentrations in sediments (A) and garden soils (B) after 20 min induction time in sediments and soils and sample process time (about 15 min).

Experimental procedures

Chemicals

Poly(allylamine hydrochloride) (PAAH, MW *c.* 70 000 Da) and poly(fluorescein isothiocyanate allylamine hydrochloride) (FITC-PAAH, MW *c.* 15 000 Da), iron(II) and iron(III) chlorides (99%) were purchased from Sigma-Aldrich. Other chemicals were obtained from Sigma-Aldrich and were analytical grade reagents. Water purified by reverse osmosis was used in all our experiments.

Bacterial strains and culture media

The whole-cell bioreporters used in this study are listed in Table 1. *Acinetobacter baylyi* ADP1 and its mutants were incubated at 30°C. Luria–Bertani (LB) medium or minimal medium (MM) (Huang *et al.*, 2005) was used for the culti-

vation of bacteria as appropriate. Briefly 1 l of MM contains 2.5 g of Na_2HPO_4, 2.5 g of KH_2PO_4, 1.0 g of NH_4Cl, 0.1 g of $MgSO_4$ $7H_2O$, 10 µl of saturated $CaCl_2$ solution, 10 µl of saturated $FeSO_4$ solution and 1 ml of Bauchop and Elsden solution (Bauchop and Elsden, 1960). MM-succinate (MMS) was prepared by the addition of 20 mM succinate to MM. As appropriate, salicylate, toluene and octadecane were added into MMS as inducers to bioreporters. ADP1 and its bioreporter mutants were grown in LB overnight at 30°C and washed by water three times before MNPs functionalization.

Synthesis of MNPs

Magnetic nanoparticles were prepared as previously describes (Fakhrullin *et al.*, 2010) with modifications. Briefly, 2.0 ml of 1 M $FeCl_3$ and 0.5 ml of 2 M $FeCl_2$ aqueous solutions were mixed and stirred vigorously, then 25 ml of 1.0 M

Table 1. Strains and plasmids used in this study.

Bacteria and plasmids	Description	Reference
Acinetobacter baylyi strains		
ADP1(BD413)	Wild type	Juni and Janik (1969)
ADPWH_lux	Bioreporter of salicylate. Promoterless *luxCDABE* from pSB417 were inserted between *salA* and *salR* genes in the chromosome	Huang *et al.* (2005)
ADPWH_alk	Bioreporter of alkanes. Promoterless *luxCDABE* were inserted in *alkM* gene in the chromosome	D. Zhang, Y. He, J. Zhao, L. Wu, J. Wang, H. Wang and W.E. Huang, in preparation
ADPWH-Pu-lux-xylR	Bioreporter toluene/xylenes, Pu fused with promoterless *luxCDABE* were inserted between *salA* and *salR* genes. *xylR* with its own promoter was inserted into *salA*. All genes were in the chromosome	Huang *et al.* (2008)

aqueous ammonia solution was added dropwise while stirring resulting in the appearance of a dark iron oxide precipitate. The precipitate was separated with a permanent magnet and washed with water until the supernatant reached pH 7. To stabilize the as-made MNPs with the cationic polyelectrolyte, 1 ml of the as-made MNPs was added into 10 ml of 10 mg ml^{-1} aqueous PAAH, sonicated for 10 min at 30% power (Branson Digital Sonifier Model 450, 5 mm tip, 400 W maximal power), then separated by centrifugation, washed with water followed by centrifugation, then re-dispersed in water and sonicated again as described above. The size distribution of the resulting MNPs was determined from TEM images. Zeta-potential (in water) of the resulting MNPs were measured using a Malvern Zetasizer 3000 instrument. To examine the deposition of MNPs on single cells, FITC-PAAH was used to stabilize MNPs and fluorescently labelled MNPs were visualized using an Olympus BX 51 epifluorescent microscope equipped with a 100× Neofluar oil immersion objective n.a. 1.3 and a DP 70 CCD camera.

Magnetization of bacterial bioreporters

The magnetic functionalization of bacterial bioreporters cells (*Acinetobacter* ADPWH_lux, ADPWH-Pu-lux-xylR and ADPWH_alk) was performed as follows. Each 1.2 ml of bioreporter cells were harvested from the overnight growth media by centrifugation, washed three times with water, then resuspended in 200 μl of water and introduced into 1 ml of aqueous PAAH-stabilized MNPs (0.4 mg ml^{-1}), followed by vortexing for 15 min. Then, the MNPs-coated cells were separated from the unbound MNPs with a permanent magnet and washed with water three times. Finally, the magnetized bacterial biosensors were resuspended in 0.85% NaCl and used in further experiments. Characterization of the magnetized bacteria was performed using various microscopy techniques. Optical footages and fluorescence microscopy images were taken using an upright Olympus BX51 microscope equipped with 50× and 100× objectives. TEM images of MNPs and ultrathin sections of resin-embedded bacteria cells and the corresponding EDX spectrum were obtained using a JEM 2011 (JEOL) transmission electron microscope (Oxford Instruments). SEM images were obtained using a Carl Zeiss Evo 60 field emission scanning electron microscope. Sample preparation involved placing 5 μl of a sample onto the acetone-wiped glass stubs, drying overnight and sputter-coating with a thin carbon film.

Functionalization efficiency and viability tests

To determine the efficiency of MNPs functionalization, ready-prepared MNPs solution was mixed with bioreporter ADPWH_lux. The MNPs-functionalized cells were harvested with a permanent magnet for 15 min and the supernatants were transferred into a new tube. The populations of magnetically functionalized and non-functionalized ADPWH_lux cells were estimated by colony-counting on LB agar plates. MFBs and non-magnetic cells were diluted using a series dilution of 10^1, 10^2, 10^3, 10^4, 10^5 and 10^6 and 100 μl diluted cells were added onto LB agar plates and incubated at 30°C for cfu counting. Six replicates were carried out for each treatment.

Bioreporters induction and bioluminescence detection

Three chromosomally based *Acinetobacter* bioreporters ADPWH_lux, ADPWH-Pu-lux-xylR and ADPWH_alk (Table 1), which are able to detect salicylate, toluene/xylenes and alkanes, were employed to test the effect of MNPs functionalization. After grown in LB at 30°C overnight, the cells of *Acinetobacter* bioreporters were harvested by centrifugation at 3000 r.p.m. for 10 min at 4°C, and subsequently washed and resuspended in 0.85% NaCl solution with the same volume. The bioreporters were stored at 4°C and were ready for use. It was reported previously that *Acinetobacter* bioreporters could remain active for at least 1 week at 4°C (Song *et al.*, 2009). Half of these cells were treated with MNPs as described above and half were used as native control cells. Salicylate stock solution (100 mM) was added into MMS to make final concentrations of 100, 10, 1, 0.1 and 0.05 μM. Toluene was added into MMS to make final concentrations of 6, 60 and 600 μM. Different chain length of n-alkanes, including octane (16.2 μl), dodecane (22.7 μl), tetradecane (26.0 μl), octadecane (33.7 mg), dispersed in 10 ml of ethanol to make 10 mM n-alkane stock solution respectively. The stock solutions were homogenized using a 40 kHz ultrasound for 10 s before use. Those alkanes were added into MMS to make final concentrations of 100 μM which should contain soluble and micro-droplet alkanes. The octadecane solution was passed through a 0.2 μm filter (Sartorius) to remove oil droplets and make clear octadecane saturated solution. Saturated octadecane solution was also added into salicylate and toluene to make 1 μM salicylate–octedecane and 30 μM toluene–octadecane mixture solutions separately.

The 200 μl mixture of cell and MMS with inducers was added into each well of a black clear-bottom 96-well micro-

plate (Fisher Scientific, UK). The microplate was incubated at 30°C and monitored for 2 h. The bioluminescence and OD$_{600}$ were measured every 10 min using Infinite M200 multimode microplate reader (TECAN Group, Switzerland) equipped with Magellan (version 6.0) analysis software. At least three replicates were carried out for each sample. To establish a calibration curve of cell population and OD$_{600}$, cells that grew at the same condition as tested samples were sampled at different OD$_{600}$, diluted, plated on LB agar plates and counted. Relative bioluminescence was obtained by dividing bioluminescence by cell population per well. Bioluminescence response ratio was calculated by dividing induced bioluminescence by relevant bioluminescence of control (non-induced) samples.

MFBs detecting salicylate in sediment and soil

Salicylate was added into river sediment and garden soil (Fig. S4) to make the final concentrations of 0.14, 1.4, 14 and 140 mg per kilogram of sediments or soils. Salicylate amended soil and sediment were stabilized for 24 h at room temperature. Each treatment was carried out in triple. One gram of soil taken from each treatment was added into 4.0 ml of water and exposed to 40 kHz ultrasound for 300 s. Five hundred microlitres of ADPWH_lux MFBs (10^9 cfu ml^{-1}) and 500 μl of LB medium were added into each sediment or soil sample. To encourage the interaction of MFBs with salicylate in sediment/soil samples, the mixture samples were incubated at 30°C for 20 min. After incubation, MNPs-functionalized ADPWH_lux were magnetically collected using a permanent magnet for 10 min from 2.0 ml of soil suspension. Subsequently, the supernatant and sediments/soils were removed carefully by pipettes. The recovered magnetic cells (1.8 ml) and 200 μl of fresh LB medium were mixed before the sample was loaded to the microplate reader.

Acknowledgements

References

Ai, H., Fang, M., Jones, S.A., and Lvov, Y.M. (2002) Electrostatic layer-by-layer nanoassembly on biological microtemplates: platelets. *Biomacromolecules* **3:** 560–564.

Andreeva, D.V., Gorin, D.A., Mohwald, H., and Sukhorukov, G.B. (2007) Novel type of self-assembled polyamide and polyimide nanoengineered shells – fabrication of microcontainers with shielding properties. *Langmuir* **23:** 9031–9036.

Atsumi, S., Higashide, W., and Liao, J.C. (2009) Direct photosynthetic recycling of carbon dioxide to isobutyraldehyde. *Nat Biotechnol* **27:** 1177–1180.

Bauchop, T., and Elsden, S.R. (1960) The growth of microorganisms in relation to their energy supply. *J Gen Microbiol* **23:** 457–469.

Berry, V., and Saraf, R.F. (2005) Self-assembly of nanoparticles on live bacterium: an avenue to fabricate electronic devices. *Angew Chem Int Edit* **44:** 6668–6673.

Corchero, J., and Villaverde, A. (2009) Biomedical applications of distally controlled magnetic nanoparticles. *Trends Biotechnol* **27:** 468–476.

Danino, T., Mondragon-Palomino, O., Tsimring, L., and Hasty, J. (2010) A synchronized quorum of genetic clocks. *Nature* **463:** 326–330.

Decher, G. (1997) Fuzzy nanoassemblies: toward layered polymeric multicomposites. *Science* **277:** 1232–1237.

Diaspro, A., Silvano, D., Krol, S., Cavalleri, O., and Gliozzi, A. (2002) Single living cell encapsulation in nano-organized polyelectrolyte shells. *Langmuir* **18:** 5047–5050.

Dobson, J. (2008) Remote control of cellular behaviour with magnetic nanoparticles. *Nat Nanotechnol* **3:** 139–143.

Dyab, A.K.F., Ozmen, M., Ersoz, M., and Paunov, V.N. (2009) Fabrication of novel anisotropic magnetic microparticles. *J Mater Chem* **19:** 3475–3481.

Fakhrullin, R.F., and Paunov, V.N. (2009) Fabrication of living cellosomes of rod-like and rhombohedral morphologies based on magnetically responsive templates. *Chem Commun* **18:** 2511–2513.

Fakhrullin, R.F., Bikmullin, A.G., and Nurgaliev, D.K. (2009) Magnetically responsive calcium carbonate microcrystals. *ACS Appl Mater Interfaces* **1:** 1847–1851.

Fakhrullin, R.F., Garcia-Alonso, J., and Paunov, V.N. (2010) A direct technique for preparation of magnetically functionalised living yeast cells. *Soft Matter* **6:** 391–397.

Gao, J.H., Gu, H.W., and Xu, B. (2009) Multifunctional magnetic nanoparticles: design, synthesis, and biomedical applications. *Acc Chem Res* **42:** 1097–1107.

Gao, L.Z., Zhuang, J., Nie, L., Zhang, J.B., Zhang, Y., Gu, N., *et al.* (2007) Intrinsic peroxidase-like activity of ferromagnetic nanoparticles. *Nat Nanotechnol* **2:** 577–583.

García-Alonso, J., Fakhrullin, R.F., and Paunov, V.N. (2010) Rapid and direct magnetization of GFP-reporter yeast for micro-screening systems. *Biosens Bioelectron* **25:** 1816–1819.

Huang, W.E., Wang, H., Huang, L.F., Zheng, H.J., Singer, A.C., Thompson, I.P., and Whiteley, A.S. (2005) Chromosomally located gene fusions constructed in *Acinetobacter* sp. ADP1 for the detection of salicylate. *Environ Microbiol* **7:** 1339–1348.

Huang, W.E., Singer, A.C., Spiers, A.J., Preston, G.M., and Whiteley, A.S. (2008) Characterizing the regulation of the Pu promoter in *Acinetobacter baylyi* ADP1. *Environ Microbiol* **10:** 1668–1680.

Juni, E., and Janik, A. (1969) Transformation of *Acinetobacter calcoaceticus* (*Bacterium anitratum*). *J Bacteriol* **98:** 281–288.

Katz, E., and Willner, I. (2004) Integrated nanoparticle–biomolecule hybrid systems: synthesis, properties, and applications. *Angew Chem Int Ed Engl* **43:** 6042–6108.

Krol, S., Nolte, M., Diaspro, A., Mazza, D., Magrassi, R., Gliozzi, A., and Fery, A. (2005) Encapsulated living cells on microstructured surfaces. *Langmuir* **21:** 705–709.

Kuo, W.S., Wu, C.M., Yang, Z.S., Chen, S.Y., Chen, C.Y., Huang, C.C., *et al.* (2008) Biocompatible bacteria@Au composites for application in the photothermal destruction of cancer cells. *Chem Commun* **37:** 4430–4432.

Ro, D.K., Paradise, E.M., Ouellet, M., Fisher, K.J., Newman, K.L., Ndungu, J.M., *et al.* (2006) Production of the antimalarial drug precursor artemisinic acid in engineered yeast. *Nature* **440:** 940–943.

Safarik, I., Rego, L.F.T., Borovska, M., Mosiniewicz-Szablewska, E., Weyda, F., and Safarikova, M. (2007) New magnetically responsive yeast-based biosorbent for the efficient removal of water-soluble dyes. *Enzyme Microb Technol* **40:** 1551–1556.

Safarikova, M., Maderova, Z., and Safarik, I. (2009) Ferrofluid modified *Saccharomyces cerevisiae* cells for biocatalysis. *Food Res Intern* **42:** 521–524.

Shutava, T.G., Balkundi, S.S., Vangala, P., Steffan, J.J., Bigelow, R.L., Cardelli, J.A., *et al.* (2009) Layer-by-layer-coated gelatin nanoparticles as a vehicle for delivery of natural polyphenols. *ACS Nano* **3:** 1877–1885.

Silva-Rocha, R., and de Lorenzo, V. (2008) Mining logic gates in prokaryotic transcriptional regulation networks. *FEBS Lett* **582:** 1237–1244.

Song, Y.Z., Li, G.H., Thornton, S.F., Thompson, I.P., Banwart, S.A., Lerner, D.N., and Huang, W.E. (2009) Optimization of bacterial whole cell bioreporters for toxicity assay of environmental samples. *Environ Sci Technol* **43:** 7931–7938.

Stricker, J., Cookson, S., Bennett, M.R., Mather, W.H., Tsimring, L.S., and Hasty, J. (2008) A fast, robust and tunable synthetic gene oscillator. *Nature* **456:** 516–519.

Veerabadran, N.G., Goli, P.L., Stewart-Clark, S.S., Lvov, Y.M., and Mills, D.K. (2007) Nanoencapsulation of stem cells within polyelectrolyte multilayer shells. *Macromol Biosci* **7:** 877–882.

Wei, H., and Wang, E. (2008) Fe_3O_4 magnetic nanoparticles as peroxidase mimetics and their applications in H_2O_2 and glucose detection. *Anal Chem* **80:** 2250–2254.

Whitesides, G.M. (2005) Nanoscience, nanotechnology, and chemistry. *Small* **1:** 172–179.

Zamaleeva, A.I., Sharipova, I.R., Porfireva, A.V., Evtugyn, G.A., and Fakhrullin, R.F. (2010) Polyelectrolyte-mediated assembly of multiwalled carbon nanotubes on living yeast cells. *Langmuir* **26:** 2671–2679.

Supporting information

Additional Supporting Information may be found in the online version of this article:

Fig. S1. The efficiency of MNPs functionalizing *Acinetobacter* strain ADPWH_lux was 99.96 ± 0.01%. Cell populations of magnetic and non-magnetic cells after MNPs functionalization were 2.22×10^8 and 8.00×10^4 respectively. The process of magnetic functionalization was biocompatible since magnetic cells were still viable and able to form colonies on LB agar plates.

Fig. S2. Dynamics of non-magnetic and magnetic *Acinetobacter* strain ADPWH_lux during 120 min incubation. Initially, all cells were magnetic. Non-magnetic free cells appeared after 30 min incubation due to bacterial division and they gradually increased to 12% at 120 min.

Fig. S3. Scanning electron microscopy (SEM) image of *Acinetobacter* ADPWH_lux bioreporters functionalized with PAAH-stabilized MNPs.

Fig. S4. Calibration curves of OD_{600} and cell population of (A) native *Acinetobacter* cells and (B) MNPs-functionalized *Acinetobacter* cells when cells were grown in MMS medium.

Fig. S5. The bioluminescence intensity (data averaged from 40 to 90 min in Fig. 4) of ADPWH_lux is proportional to the concentration of salicylate in sediments (A) and soils (B) in the range of 0–14 mg per kg of samples.

Movie S1. A real-time optical microscopy footage illustrating the magnetically-facilitated movement of MNPs-functionalized bacteria cells.

Please note: Wiley-Blackwell are not responsible for the content or functionality of any supporting materials supplied by the authors. Any queries (other than missing material) should be directed to the corresponding author for the article.